Modeling Wet-Snow Shedding from Current-Carrying Conductors

Ossama Olqma[1], László E. Kollár[1], Masoud Farzaneh[1], Laure Pellet[2]

[1]NSERC/Hydro-Québec/UQAC Industrial Chair on Atmospheric Icing of Power Network Equipment (CIGELE) and
Canada Research Chair on Atmospheric Icing Engineering of Power Networks (INGIVRE) http://www.cigele.ca
at Université du Québec à Chicoutimi, Chicoutimi, QC, Canada

[2]Électricité de France (EDF), Recherche & Développement, Clamart, France

Abstract—**The initiation of wet-snow shedding from current-carrying conductors was studied experimentally and theoretically. A suspended cable with cylindrical snow accretion was considered, and some of the snow properties at the end of sleeve were measured and calculated until snow shedding. The current in the cable appears to be a heat source which accelerates snow melting, similarly to air temperatures above freezing, wind and heat radiation. All of these effects were taken into account to study how they contribute to the snow-shedding process. The properties observed were the liquid water content, density, and profile of snow at the end of a snow sleeve. As the snow warms, if the liquid water content and density increase to high enough levels, adhesion to the cable is weakened so that the end of the snow sleeve turns downward and then falls off. The experimental procedure involved forming a wet-snow sleeve on a suspended cable with negligible sag, frequently measuring snow properties of interest under controlled ambient conditions, and observing the deformation of the snow-sleeve until shedding occurred. The theoretical model applies the heat balance of the snow sleeve to calculate the effects of the heat sources mentioned, and simulates water percolation in the cross-section at the end of the snow sleeve from the top half downward. The model provides the rate of increase of liquid water content and density of snow in the end section, and predicts the deflection of the same section together with the time when this section is detached from the cable and snow sheds. The theoretical results were compared to the experimental observations, and satisfactory coincidence was observed in most of the cases examined.**

I. Introduction

WET snow adheres strongly to exposed objects and the accretion may grow and persist for a long time on overhead transmission lines under favorable conditions. The accumulated snow creates a vertical load on the line, whereas the shedding snow results in unbalanced forces. Therefore, predicting the duration of snow persistence on the cable and understanding the initiation and propagation of wet-snow shedding are particularly important from the point of view of line design. The presence of liquid water in the snow matrix is essential for strong adhesion; however, a high amount of liquid water weakens the cohesive and adhesive forces, and leads to snow shedding when these forces are overcome by gravity and wind. Natural thermodynamic effects such as heat convection due to wind with air temperatures above the freezing point or solar radiation lead to an increase in the liquid water content (LWC) of snow, but the process of snow shedding may further be accelerated when current-carrying conductors are heated by Joule effect.

Wet-snow accretion and shedding on overhead wires was observed mainly in Japan [1], France [2, 3] and Iceland [4], although this phenomenon is not limited to these countries. Snow shedding was also observed in wind tunnel experiments when studying wet-snow accretion [1, 5]. The main findings of former experiments and observations on wet-snow shedding are summarized in [6].

Snow shedding has been examined in several recent studies at CIGELE. References [7, 8] proposed a simple and innovative method to reproduce snow sleeves in laboratory. A two-dimensional (2D) thermodynamic model to simulate snow shedding at the end section of a snow sleeve was developed in [9] and [10], and some natural effects on the process of snow shedding were studied theoretically and experimentally. Reference [11] examined experimentally snow shedding from sagged cables due to natural effects. The research of [12] was devoted to the dependence of snow adhesion to cable surfaces on snow LWC and cable surface quality. The Joule effect on ice shedding formed the subject of several previous projects [13-15], whereas an attempt is made here to simulate snow shedding from current-carrying conductors with negligible sag. The method of [7] and [8] is applied in the experimental study to prepare a snow sleeve; whereas the model of [9] is used to predict snow shedding by numerical simulation. This model simulates how LWC and density of snow vary over time, considers water migration toward the bottom at the end section of the snow sleeve, and predicts when this section turns underneath the cable and sheds.

II. Experimental Procedure and Conditions

The experimental snow sleeve was modeled on a 5-m-long cable (ALCAN Pigeon ACSR) with a diameter of 12.75 mm suspended with negligible sag in a cold chamber of the CIGELE laboratories. The experiments were carried out during a winter period, since wet snow was obtained from dry snow available outdoors. The dry snow was spread in the cold chamber at a temperature above freezing until the snow became wet enough to stick to the cable after compression. This meant an initial LWC of 10-15 % by mass in the snow sleeve. Although snow

quality was checked regularly, the LWC was sometimes out of this required range since it was difficult to estimate what the LWC would be after the snow was compressed to form a sleeve. The wet snow was placed in a semi-cylindrical mold set below the cable, and then it was compressed using a semi-cylindrical hand tool [7, 8]. The resulting snow sleeve with a diameter of 9.5 cm was obtained after the mold removal, as shown in Fig. 1.

Fig.1. Snow sleeve on the suspended cable at the beginning of an experiment (the removed mold can be seen on the right side of the snow sleeve)

The room temperature was controlled and kept constant during the experiments, between 1 °C and 5 °C. It was also possible to generate low-speed wind and simulate heat radiation by halogen lamps in the cold chamber. The effects of these parameters were examined in [9] and [10]. This study focuses on the effects of current in the cable, which is produced by a generator (see Fig. 2). The current was varied up to 100 A under different ambient conditions, and an additional test was conducted at 250 A.

Fig. 2. The generator and its connection to the cable

Several variables were measured during the experiments: LWC and density of snow from time to time at the end section of snow sleeve, deformation of the same section, and time until snow shedding. The LWC was measured using the melting calorimetry method. Details of measurement and error analyses are provided in [9] and [10]. The density of snow was simply obtained by measuring the mass of snow samples taken with a cylindrical piece of known volume. The deformation of the end section was recorded by taking photos.

III. Modeling

Research on snow shedding from suspended cables is not as advanced as that of ice shedding, but some wet-snow accretion models have been developed [16-19]. These apply a condition for snow shedding: when the LWC reaches 40 %, then the snow sleeve breaks up and sheds before its diameter could grow high enough to be dangerous for the transmission line. The LWC was expressed in these models as a percentage of the mass of liquid water divided by the total mass of snow, as will be the case herein. The above-mentioned models are based on heat balance. A similar approach was used in [9] and [10] to simulate snow shedding. The authors constructed a 2D thermodynamic model; however, contrarily to the accretion models, precipitation was not assumed, but the effects of solar radiation were considered. Furthermore, this model takes into account water transfer toward the bottom of the snow sleeve. Since this model is used in this study, a brief description is provided as follows.

First, the model uses heat balance to determine the mass of melted water in the vertical section at the end of a snow sleeve on a cable with negligible sag. Thus, the average LWC and density of the section may be determined. Then, water percolation is simulated assuming that no water dripping occurs, and LWC and density variations are calculated for the fractions of the snow sleeve end section which are above and below the line passing through the midpoint of the cable, which will hereafter be called cable centerline. The model also predicts to what extent the end section is deflected; and when the whole section moves below the centerline, shedding is assumed to have occurred and simulation is terminated.

A. Heat Balance

The terms in the heat balance of the snow sleeve, which provide the latent heat, Q_f (W), to melt the snow are the convective heat, Q_c (W), the heat transfer due to evaporation or condensation, Q_e (W), the heat gained from radiation, Q_r (W), and the heat generated by the current, Q_J (W):

$$Q_f = Q_c + Q_e + Q_r + Q_J \qquad (1)$$

Since no accumulation is assumed during the process simulated, the heat required to melt the snow is simply calculated as follows:

$$Q_f = L_f \frac{\mathrm{d}M_f}{\mathrm{d}t} \qquad (2)$$

where M_f (kg) is the mass of melted water within the snow matrix, t (s) is time, and $L_f = 3.35 \times 10^5$ J/kg is the latent heat of fusion.

The convective heat transfer between the ambient air and the snow layer is expressed by

$$Q_c = hA_c(T_a - T_s) \tag{3}$$

with $h\ \left(\text{W}/\left(\text{m}^2 \times \text{K}\right)\right)$ standing for heat transfer coefficient, $A_c\ \left(\text{m}^2\right)$ denoting the circumferential surface area of exchange, whereas $T_a\ (^{\circ}\text{C})$ and $T_s\ (^{\circ}\text{C})$ denote the temperatures of the air and snow surface, respectively. The heat transfer coefficient is related to the Nusselt number, Nu, as follows:

$$h = \frac{k_a \text{Nu}}{D} \tag{4}$$

where $k_a = 2.42 \times 10^{-2}$ W/(m × K) is the thermal conductivity of air, and D (m) is the diameter of accreted snow. The Nusselt number is calculated by one of the following formulae:

$$\text{Nu}_{fr} = 0.525(\text{GrPr})^{1/4} \tag{5}$$

for free convection as proposed by [20], or

$$\text{Nu}_{fo} = 0.032 \text{Re}^{0.85} \tag{6}$$

for forced convection following the recommendation of [21]. The non-dimensional parameters are the Grashof number, $\text{Gr} = g\beta_a(T_a - T_s)D^3/v_a^2$, Prandtl number, $\text{Pr} = \mu_a c_p/k_a$, and Reynolds number, $\text{Re} = \rho_a U_a D/\mu_a$, with the parameters, $g = 9.81$ m/s^2, gravitational constant, $\beta_a = 1/((T_a + T_s)/2)$, thermal expansion coefficient of air, $v_a = 1.34 \times 10^{-5}$ m^2/s and $\mu_a = 1.73 \times 10^{-5}$ kg/(m × s), kinematic and dynamic viscosity of air, respectively, $c_p = 1006$ J/(kg × K), specific heat of air at constant pressure, $\rho_a = 1.28$ kg/m^3 is air density, and U_a (m/s) is wind speed.

The heat transfer due to evaporation of liquid water or condensation of water vapor is obtained from the formula:

$$Q_e = M_{w,a}\left(\frac{\text{Pr}}{\text{Sc}}\right)^{0.63}\frac{L_v}{c_p}hA_c\frac{\Delta e_w}{p} \tag{7}$$

where $M_{w,a} = 0.622$ is the ratio of the molar weights of water vapor and air, $\text{Sc} = v_a/D_{w,a}$ is the Schmidt number, $D_{w,a} = 2.1 \times 10^{-5}$ m^2/s is the diffusion coefficient of water vapor in air, $L_v = 2.5 \times 10^6$ J/kg is the latent heat of vaporization, $p = 101325$ Pa is the atmospheric pressure, and $\Delta e_w = \varphi e_w(T_a) - e_w(T_s)$ is the difference between vapor pressure in the air and at the snow surface, with $e_w(T)$ (Pa) and φ denoting saturation vapor pressure at temperature T and relative humidity of air, respectively. The relative humidity of air was assumed constant in the experiments: $\varphi = 0.8$.

The heat transfer due to radiation is the sum of short- and long-wave radiations:

$$Q_r = (1 - \alpha)I_r A_r + \varepsilon\sigma_R(T_a^4 - T_s^4)A_c \tag{8}$$

The intensity, $I_r\ \left(\text{W}/\text{m}^2\right)$, is obtained from the value measured in lx divided by the product of 683 lm/W and the luminous efficiency of the halogen lamp, which was taken to be 3.5 %. The radiated surface, $A_r\ \left(\text{m}^2\right)$, is the projection of the sleeve surface in the plane perpendicular to radiation. The albedo of wet snow, α, is set at 0.6 [22], whereas the emissivity of snow, ε, is equal to 0.98 [23]. The $\sigma_R = 5.57 \times 10^{-8}$ W/(m^2 × K^4) is the Stefan-Boltzmann constant, and the temperature of chamber walls is assumed to be equal to the air temperature, $T_a\ (^{\circ}\text{C})$.

The heat due to Joule effect is produced by the current carried in the cable, I, and also depends on the electric resistance of the cable, R, which is 2 mΩ in this case:

$$Q_J = RI^2 \tag{9}$$

B. Water Percolation and Deflection of End Section

LWC and density are assumed to be constant initially in the cross section of the snow sleeve. Then, once the water distribution in snow is in funicular mode, the liquid water begins to migrate from top to bottom. If, for the sake of simplicity, the capillary influence on water flow is ignored, then the flow occurs under the effect of gravity, and can thus be described by the simplified form of Darcy's law [24]. The size of the cavity which is developing underneath the cable is determined from this water flow, and thus, the deflection of the end section may be obtained. The LWC and density in the fractions of the snow sleeve end section, which are above and below the cable centerline, are calculated after considering the following phenomena: (i) the sleeve mass is constant, because the evaporated mass is negligible; thus, snow melting causes an increase in density and a reduction of sleeve diameter; (ii) snow melting increases the LWC everywhere; (iii) snow mass decreases above the cable centerline and increases below the cable centerline due to the deflection of end section; (iv) water mass decreases above the cable centerline and increases below the cable centerline due to water percolation. The calculation continues until the entire end section turns below the cable centerline, then shedding is assumed and computation is terminated. The details of the computation summarized in this section are provided in [9] and [10].

IV. RESULTS AND DISCUSSION

A. Shedding Mechanism

The experimental observations herein show that snow shedding always begins at the end of the snow sleeve when the cable sag is negligible. Different shedding mechanisms were observed from cables with considerable sag [11]. Initially, the snow sleeve is homogeneous; its circumference is concentric with the cable. Later, the bottom part of the sleeve becomes more and more transparent, as water migrates downward. Simultaneously, the end section begins to turn down, and a zone of cavity appears below the cable. Approaching the end

of the shedding process, the entire

TABLE 1: EXPERIMENTAL RESULTS WITH VARYING CURRENT IN THE CABLE (NO WIND, NO RADIATION), TIME IN PARENTHESES BELOW FINAL DENSITY DATA INDICATES TIME OF LAST DENSITY MEASUREMENT

T_a (°C)	I (A)	Initial LWC (%)	Initial density (kg/m^3)	Final LWC (%)	Final density (kg/m^3)	Shedding time (h:min)	Average slope (% / h)
3	0	13.0	510	33.7	830 (7:20)	7:20	2.3
3	50	17.6	420	47.4	650 (2:00)	2:35	12.1
3	100	13.6	510	52.1	750 (2:00)	2:15	15.7
3	250	12.0	330	34.7	430 (0:30)	0:40	29.8

end section turns underneath the cable, and water droplets may start dripping from the tip of the section. The process ends with the shedding of a snow chunk 20 cm to 30 cm in length. Since the time when water dripping was observed is very short as compared to the whole duration of the process, the theoretical model stops when the entire end section turns underneath the cable, so that water dripping is not considered in the model. The main difference between the shedding mechanisms with and without current in the cable is that the cavity below the cable develops along the whole sleeve when the cable carries current, but it is still the greatest at the end of the sleeve, and shedding begins there. A more detailed description of the shedding mechanism can be found in [9] and [10].

B. Effects of Current on Snow Shedding

Four parameters, (i) air temperature, (ii) wind speed, (iii) heat radiation, and (iv) current in the cable, were varied in the experiments as explained in Section II. Natural effects, i.e. the effects of the first three parameters were examined in [10]; whereas the influence of cable current is discussed here. The LWC and density at one end of the sleeve together with time were measured regularly until snow shed from the other end.
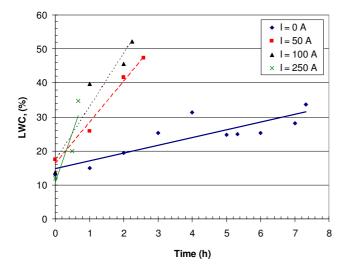

Fig.3. Time histories of LWC until snow shedding with current as parameter, $T_a = 3\,°C$, no wind, no radiation

Table 1 and Fig. 3 summarize the results of some experiments with varying current and other parameters unchanged. In these experiments, wind and heat radiation were not simulated, therefore Table 1 shows the values of the other

two adjusted parameters: air temperature and cable current; along with the measured parameters: initial and final LWCs and densities, shedding time, and average slope describing the increase in LWC at the end section in time (slope of the linear fit on measured data points such as the lines shown in Fig. 3). Density measurements require a large enough unbroken piece of snow, which was not always available after shedding; therefore, the time in parentheses appearing below the final density data indicates when the last density measurement took place. The ranges of LWC and density as measured in the moment of shedding approximately correspond to those measured in the experiments without current [10]. The only exception is the density at the end of the test at 250 A, where the shedding process is the fastest observed, and density may increase significantly even in a short time, and this low value may have been measured due to non-homogeneity in the sleeve.

Figure 3 clearly illustrates to what extent the application of current in the cable accelerates the shedding process. A current of 50 A rises the slope of increase in LWC and reduces shedding time significantly. If the current is 250 A, then a more than tenfold increase in the slope and decrease in time may be observed.

C. Comparison of the Effects of Current and Ambient Parameters

The effects of heating the cable by current and the effects of natural processes are compared in Fig. 4. This figure shows experimentally obtained time histories of LWC until shedding for a basic case (air temperature slightly above freezing
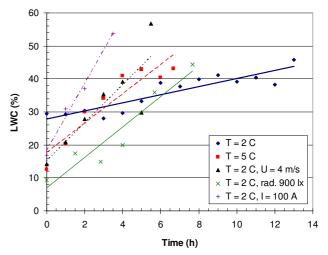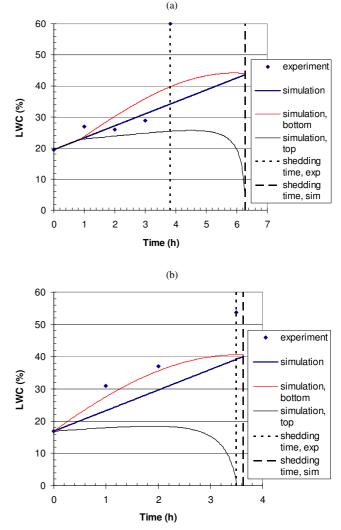
Fig. 4. Time histories of LWC showing the effects of four parameters: air temperature (*T*), wind speed (*U*), heat radiation, and current in the cable (*I*)

($2°C$), no wind, no radiation, no current), and for four other cases where one parameter is modified with respect to the basic case. The influence of each parameter may be observed in the slope of LWC increase and in the shedding time. A $3°C$ increase in the air temperature and the application of heat radiation due to 900 lx illumination have considerable effects on snow shedding, but a low-velocity wind (4 m/s) will accelerate the shedding process even more. A current of 100 A in the cable has the greatest influence among all the parameters considered in this analysis.

D. Comparison of Experimental and Simulation Results

This section presents the results obtained from the thermodynamic model described in Section III, and compares them to experimental observations. The time step of computation was chosen to be one minute. The model calculates the average LWC in the whole section at the end of the snow sleeve, and in the top and bottom parts of the same section. The corresponding curves are shown in Fig. 5 with labels "simulation", "simulation, top" and "simulation, bottom", respectively. The LWC increases by the same extent in the top and bottom parts of the sleeve at the beginning of most of the simulations (as shown in Fig. 5a), because the water distribution in the snow matrix is in pendular mode and water percolation does not occur. When water transfer begins, the three curves become separated, because the LWC increases faster in the bottom than in the top part of the sleeve, and because the end section starts to turn down. The LWC value approaches zero, in the top part, and its value in the bottom part approaches the average LWC of the entire section, because the top part will disappear and the whole section will be in the bottom by the end of the simulation.

Figures 5a and 5b show both simulation and experimental results for currents of 50 A and 100 A, respectively, when further parameters are unchanged: air temperature is $2°C$, and no wind and no radiation are simulated. Since the top part of the sleeve turns downward quite quickly in the experiments with current, only one sample from the bottom part was taken at each measurement. The "simulation, bottom" curve follows closely the measurement points in Fig. 5; although the last measurement points are significantly above the simulation curves. However, the reliability of the LWC measurement of the shed snow sample is questionable, because the snow was slushy and melted quickly. Thus, the measured LWC overestimates the real values by a few percentage points. The model provides a close approximation or a slight underestimation of the shedding time when current is not carried in the cable [9, 10]. A close approximation may also be observed in Fig. 5b; however, the shedding time is overestimated by the model in the case presented in Fig. 5a. A plausible explanation of this fact is that a cavity below the cable develops everywhere along the sleeve when the cable carries current, which may additionally accelerate the shedding

process and which is not considered in the model. The reader is referred to [9] for further results and explanations.

Fig. 5. Measured (experiment) and calculated (simulation) LWC time histories, (a) $T = 2°C$, $I = 50$ A; (b) $T = 2°C$, $I = 100$ A

V. CONCLUSIONS

The research described herein studied wet-snow shedding from a suspended cable with negligible sag. The shedding mechanism was simulated in cold-chamber experiments, and a 2D thermodynamic model was constructed to predict the variation of snow properties at the end section of the snow sleeve until shedding. In particular, the effects of current in the cable were examined, but further parameters, including air temperature, wind speed and heat radiation, were also varied. The contribution of these parameters to snow shedding was compared, and this comparison revealed that a current of 100 A accelerates the shedding process more than any of the other parameters. It should be noted, however, that this value was obtained in small-scale experiments; hence, the current should be different in a real-scale transmission line. The model predicts satisfactorily the rate of LWC increase and shedding time in most of the cases simulated. The model does not consider the fact that when the cable carries current, a cavity

develops underneath the cable, along the whole sleeve. Although the cavity is still the greatest at the end of sleeve and shedding begins there, shedding time may be reduced. This fact causes the overestimation of shedding time by the model in some cases. A challenging problem yet to be solved is the development of a 3D model which takes into account heat transfer in the whole snow sleeve. Such a model would improve predictions and would also be applicable to simulate snow shedding from cables with considerable sag.

VI. Acknowledgments

VII. References

[1] G. Wakahama, D. Kuroiwa, and K. Goto, "Snow Accretion on Electric Wires and its Prevention," *Journal of Glaciology,* vol. 19, no. 81, pp. 479-487, 1977.

[2] P. Admirat, J. L. Lapeyre, and B. Dalle, "Synthesis of Filed Observations and Practical Results of the 1983-1990 "Wet-Snow" Programme of Electricité de France," in *Proc. 5th International Workshop on Atmospheric Icing of Structures*, Tokyo, Japan, 1990, pp. B6-2-(1) - B6-2-(5).

[3] P. Admirat, and J. L. Lapeyre, "Observation d'accumulation de neige collante à la station de Bagnères de Luchon les 6, 7 avril 1986 - Effet préventif des contrepoids antitorsion", EDF-DER HM/72-5535, 1986.

[4] A. J. Eliasson, and E. Thorsteins, "Field Measurements of Wet Snow Icing Accumulation," in *Proc. 9th International Workshop on Atmospheric Icing of Structures*, Chester, England, 2000.

[5] Y. Sakamoto, P. Admirat, J. L. Lapeyre, and M. Maccagnan, "Thermodynamic simulation of wet snow accretion under wind-tunnel conditions," in *Proc. 4th International Workshop on Atmospheric Icing of Structures*, Paris, France, 1988, pp. A6.6.

[6] Y. Sakamoto, S. Tachizaki, and N. Sudo, "Snow Accretion on Overhead Wires," in *Proc. 11th International Workshop on Atmospheric Icing of Structures*, Montreal, QC, Canada, 2005, pp. 3-9.

[7] M. Roberge, "A Study of Wet Snow Shedding from an Overhead Cable," M.Eng. thesis, Department of Civil Engineering and Applied Mechanics, McGill University, Montreal, QC, 2006.

[8] M. Roberge, M. Farzaneh, G. McClure, and C. Peyrard, "Wet Snow Shedding from an Overhead Cable. Part I: Experimental Study," in *Proc. 12th International Workshop on Atmospheric Icing of Structures*, Yokohama, Japan, 2007.

[9] O. Olqma, "Critères de déclenchement du délestage de la neige collante de câbles aériens (Criteria for Initiation of Snow Shedding from Overhead Cables, in French)," M.Eng. thesis, Department of Applied Sciences, University of Quebec at Chicoutimi, Chicoutimi, QC, submitted in 2009.

[10] L. E. Kollár, O. Olqma, and M. Farzaneh, "Natural Wet-Snow Shedding from Overhead Cables," *Cold Regions Science and Technology*, accepted in 2009.

[11] A. Fonyó, L. E. Kollár, M. Farzaneh, and P. Montpellier, "Experimental Simulation of Wet-Snow Shedding from Sagged Cables," in *Proc. 13th International Workshop on Atmospheric Icing of Structures*, Andermatt, Switzerland, 2009.

[12] R. Hefny, L. E. Kollár, M. Farzaneh, and C. Peyrard, "Adhesion of Wet Snow to Different Cable Surfaces," in *Proc. 13th International Workshop on Atmospheric Icing of Structures*, Andermatt, Switzerland, 2009.

[13] A. Bouamoul, "Étude expérimentale et théorique sur le processus de délestage par fonte de la glace accumulée autour d'un cylindre," Ph.D. dissertation, Departement of Applied Sciences, University of Quebec at Chicoutimi, Chicoutimi, QC, Canada, 2002.

[14] Z. Péter, M. Farzaneh, and L. I. Kiss, "Power line conductor icing prevention by theJoule effect: parametric analysis and energy requirements," in *Proc. 11th International Workshop on Atmospheric Icing of Structures*, Montreal, QC, Canada, 2005, pp. 361-372.

[15] Z. Péter, M. Farzaneh, and L. I. Kiss, "Assessment of the current intensity for preventing ice accretion on overhead conductors " *IEEE Transactions on Power Delivery,* vol. 22, no. 1, pp. 565-574, 2007.

[16] P. Admirat, M. Maccagnan, and B. D. Goncourt, "Influence of Joule effect and of climatic conditions on liquid water content of snow accreted on conductors," in *Proc. 4th International Workshop on Atmospheric Icing of Structures*, Paris, France, 1988.

[17] G. Poots, and P. L. I. Skelton, "Simple models for wet-snow accretion on transmission lines: snow load and liquid water content," *International Journal of Heat and Fluid Flow,* vol. 15, no. 5, pp. 411-417, 1994.

[18] G. Poots, and P. L. I. Skelton, "Thermodynamic models of wet-snow accretion: axial growth and liquid water content on a fixed conductor," *International Journal of Heat and Fluid Flow,* vol. 16, no. 1, pp. 43-49, 1995.

[19] Y. Sakamoto, "Snow accretion on overhead wires," *Phil. Trans. R. Soc. Lond. A,* vol. 358, pp. 2941-2970, 2000.

[20] R. B. Bird, W. E. Stewart, and E. N. Lightfoot, *Transport Phenomena*, New York, NY, USA: John Wiley & Sons Inc., 1960.

[21] L. Makkonen, "Modeling of Ice Accretion on Wires," *Journal of Climate and Applied Meteorology,* vol. 23, no. 6, pp. 929-938, 1984.

[22] D. H. Male, and D. M. Grey, "Snowcover Ablation and Runoff," *Handbook of Snow*, D. M. Grey and D. H. Male, eds., Toronto, ON: Pergamon Press, 1981.

[23] K. Y. Kondratyev, *Radiation in the Atmosphere*, New York, NY: Academic Press, 1969.

[24] S. C. Colbeck, "A Theory of Water Percolation in Snow," *Journal of Glaciology,* vol. 11, no. 63, pp. 369-385, 1972.